Cancer Chemother Pharmacol (2008) 62:1045–1054
DOI 10.1007/s00280-008-0695-9

ORIGINAL ARTICLE

Pharmacokinetic profile of the microtubule stabilizer patupilone in tumor-bearing rodents and comparison of anti-cancer activity with other MTS in vitro and in vivo

Terence O'Reilly · Markus Wartmann · Joseph Brueggen · Peter R. Allegrini · Andreas Floersheimer · Michel Maira · Paul M. J. McSheehy

Received: 6 December 2007 / Accepted: 25 January 2008 / Published online: 27 February 2008

Abstract
Introduction Patupilone is a microtubule stabilizer (MTS) currently in clinical development. Here, we evaluate the anti-cancer activity in vitro and in vivo in comparison to paclitaxel and describe the pharmacokinetics (PK) of patupilone in tumor-bearing nude mice and rats.
Methods The potency in vitro of patupilone and two other MTS, paclitaxel and ixabepilone, was determined using human colon carcinoma cell lines with low (HCT-116, HT-29, RKO) and high (HCT-15) P-glycoprotein expression (P-gp), as well as two multi-drug resistance (MDR) model cell pairs, MCF7/ADR and KB-8511 cells and their respective drug-sensitive parental counterparts. The PK of patupilone was investigated in nude mice bearing HCT-15 or HT-29 xenografts and in rats bearing s.c. pancreatic CA20498 tumors or A15 glioma tumors. Anti-cancer activity in vivo was compared to that of paclitaxel using three different human tumor colon models. The retention and efficacy of patupilone was compared in small and large HT-29 xenografts whose vascularity was determined by non-invasive magnetic resonance imaging.
Results Patupilone was highly potent in vitro against four different colon carcinoma cell lines including those showing multi-drug-resistance. In contrast, paclitaxel and ixabepilone displayed significantly reduced activity with markedly increased resistance factors. In both rats and mice, a single i.v. bolus injection of patupilone (1.5–4 mg/kg) rapidly distributed from plasma to all tissues and was slowly eliminated from muscle, liver and small intestine, but showed longer retention in tumor and brain with no apparent elimination over 24 h. Patupilone showed significant activity against three human colon tumor models in vivo, unlike paclitaxel, which only had activity against low P-gp expressing tumors. In HT-29 tumors, patupilone activity and retention were independent of tumor size, blood volume and flow.
Conclusions The high potency of patupilone, which is not affected by P-gp expression either in vitro or in vivo, and favorable PK, independent of tumor vascularity, suggest that it should show significant activity in colorectal cancer and in other indications where high P-gp expression may compromise taxane activity.

Keywords Patupilone · Pharmacokinetics · Colon cancer · P-glycoprotein · Tumor vasculature

T. O'Reilly · M. Wartmann · J. Brueggen · A. Floersheimer · M. Maira · P. M. J. McSheehy (✉)
Oncology Research,
Novartis Institutes for BioMedical Research,
Novartis Pharma AG, Basel 4002, Switzerland
e-mail: paul_mj.mcsheehy@novartis.com

P. R. Allegrini
Global Imaging Group, Oncology Research,
Novartis Institutes for BioMedical Research,
Novartis Pharma AG, Basel 4002, Switzerland

Introduction

Patupilone, also known as epothilone B (EPO906) is a potent microtubule stabilizer, which is currently in phase-III clinical development for second-line ovarian cancer. Epothilones, which are secondary metabolite macrolides produced by the myxobacterium *Sorangium cellulosum* [1], represent a novel class of non-taxane microtubule-stabilizing natural products. Although patupilone has the same molecular target and binding-site as the taxanes, it binds β-tubulin with a higher affinity than paclitaxel or docetaxel [2, 3]. Binding promotes polymerization of tubulin α, β heterodimers into microtubule polymers, stabilizes

microtubules against depolymerization and suppresses microtubule dynamics, which results in mitotic cell cycle perturbation and eventual cell death by mechanisms that include induction of apoptosis in vitro [4, 5] and in vivo [6]. Preclinical work has shown that patupilone is the most active variant among the natural epothilones and is more potent than paclitaxel [7], but unlike paclitaxel is not a significant substrate of the P-glycoprotein (P-gp) drug efflux transporter encoded by the *mdr-1* gene [8]. Most importantly, patupilone has been shown to retain activity in vitro against paclitaxel-resistant cancer cells over-expressing P-gp or bearing β-tubulin mutations [7, 9]. In addition to targeting the tumor cells directly, patupilone may also kill tumor cells in vivo indirectly by targeting the vasculature of the solid tumor, since rapidly proliferating and relatively immature endothelial cells have a strong dependence on tubulin in maintaining their shape [10]. Support for this hypothesis has been provided experimentally with cultured cells using low doses of patupilone [11] and on clinical tumor explants [12] and in vivo using well-vascularised syngeneic tumor models [6]. Inhibition of endothelial cell function would also impact negatively on the metastatic process [6]. Thus, patupilone is considered to have strong potential for the treatment of solid tumors and phase-II clinical trials are ongoing [13].

Chemotherapy remains the primary treatment modality for colorectal cancer (CRC), and although improvements are being achieved, new agents are needed [14]. Recently, patupilone showed encouraging activity in CRC in a phase-1 study [15], an indication where the taxanes have failed to show activity [16], most likely reflecting the elevated levels of P-gp in normal and cancerous gut [17]. The current study summarizes pre-clinical data on the efficacy of patupilone in comparison to the taxane paclitaxel on human colon cancer cells, both in culture and grown as solid tumors in nude mice. In addition, the pharmacokinetics of patupilone in nude mice and rats are presented, which demonstrate a rapid and wide distribution of the drug to all tissues including brain and tumor, independent of tumor size and vascularity, followed by a long retention in the tumor tissue. These properties suggest that patupilone should be an effective treatment for CRC and other indications with P-gp over-expression such as renal cell carcinoma (RCC) and brain-tumors [16–19].

Materials and methods

Materials

All cell culture materials were obtained from Gibco (Paisley, Scotland) or Bioconcept (Allschwill, Switzerland). Eserine (physostigmine hemosulfate) was obtained from Sigma, Buchs, Switzerland. GdDOTA, the extra-vascular contrast agent (CA), and Endorem (dextran-coated iron oxide nanoparticles), the intra-vascular CA, were obtained from Guerbet SA, France.

Anti-cancer drugs

Patupilone (EPO906, epothilone B) and the lactam-analog of epothilone B (ixabepilone, BMS-247550) were prepared by the Chemical Department, Novartis (Basel, Switzerland) by fermentation and semi-synthesis, respectively, and stored as a dry powder at −20°C. Paclitaxel was obtained from Sigma (T1912) as a powder and stored at 4°C.

For studies in vitro, stock solutions were prepared at a final concentration of 10 mM in 100% DMSO, and small aliquots stored at −20°C. Working solutions were prepared by serially diluting thawed stocks in DMSO, followed by dilution into cell culture medium leading to a final concentration of DMSO of 0.1%.

Cell lines

The human breast carcinoma cell line MCF-7/ADR, an adriamycin-selected MDR subline of MCF-7 shown to overexpress P-gp [20], was obtained from Dr. D. Fabbro (Novartis Pharma AG, Basel, Switzerland). The human cervical adenocarcinoma line KB-31, which is effectively HeLa [21] and its colcemid-selected, P-gp overexpressing MDR derivative KB-8511 were obtained from Dr. R. M. Baker (Roswell Park Memorial Institute, Buffalo, NY, USA) and have been previously described [22]. High P-gp expression in HCT-15 relative to HT-29 > HCT-116 > MCF-7 has been reported by Wu et al. [23]. The rat glioma cell line A15 (aka 1A2R) was obtained from the European cell culture collection. All other cell lines were obtained from the American type culture collection.

IC50 determinations

Cells were cultured at 37°C in an incubator with a 5% v/v CO_2 and 80% relative humidity atmosphere. Inhibition of monolayer cell proliferation by test compounds was assessed by quantification of protein content of fixed cells by methylene blue staining as previously described [24], except that cell lines were cultured in RPMI-1640 (complemented with 10% FCS, penicillin (100 IU/ml), streptomycin (100 µg/ml) and L-glutamine (2 mM) from cell stocks previously adapted to growth in this medium. IC50 values were determined by mathematical curve-fitting using XLfit-software (IDBS, Guilford, UK) and are defined as the drug concentration, which at the end of the incubation period led to 50% inhibition of net cell mass increase compared to DMSO-treated control cultures.

Animals and tumor models

All animal experiments were performed in strict adherence to the Swiss law for animal protection. Mice and rats were identified by ear markings and kept in groups of ten or three animals, respectively, under normal conditions with access to food and water ad libitum. Female Harlan athymic nude mice weighing 20–25 g were obtained from Novartis internal breeding stocks in Basel, Switzerland. Female Balb/c mice, male Lewis rats and female BDix rats (160–200 g) were purchased from Iffa Credo (L'Abresque, France).

Solid tumors in nude mice were created either by s.c. injection of cells ($2–5 \times 10^6$ in 100 µl PBS) or transplantation using 25 mm^3 tumor fragments from donor mice. Tumor volumes (TVol) were determined by measuring three dimensions using calipers and applying the formula $l \times w \times h \times \pi/6$. Once the tumors had reached at least 100 mm^3, the mice were randomized into different treatment groups. Solid tumors in Lewis rats were created by a s.c. injection of a suspension of rat pancreatic CA20948 tumor cells from donor rats, as previously described [25]. Solid tumors in BDix rats were created by s.c. injection of 1×10^6 cells in 50 µl PBS in the flank of female rats.

The animals were treated with either patupilone or paclitaxel using i.v. bolus injections. Patupilone was dissolved in 100% PEG-300 at 1 mg/ml and diluted in 0.9% normal saline at a ratio of one part PEG-300 to two parts saline just prior to injection using 5 ml/kg in mice and 2 ml/kg in rats at doses of 1.5–4 mg/kg weekly (qw) or once only. The patupilone doses were determined from earlier experiments and represent the optimal dose in efficacy and tolerability in a particular model. Note that a dose of 1.5 mg/kg in rats and 3 mg/kg in mice is the same in mg/m^2. Paclitaxel was freshly made for each administration by dissolving in a mixture of 65% cremophor and 35% ethanol before diluting 1:4 in 0.9% saline and injecting 6 ml/kg every other day (q2d) at a dose of 15 mg/kg. The paclitaxel dose used was determined to be optimal in efficacy and tolerability as previously described [26].

The anti-tumor effect of chemotherapy was quantified at the end of the experiment (normally 2 weeks from initiation of treatment) by using the mean change (Δ) in TVol of individual mice (final value minus starting value in mm^3) as the T/C_{TVol} i.e. $\Delta TVol_{drug}/\Delta TVol_{vehicle}$.

The toxicity of chemotherapy was assessed to provide both the percentage change in BW (Δ%BW) and the fractional change ($\Delta F - BW$) in BW: $BW_{(endpoint)}/BW_{(day\ 0)}$, which was used to determine the T/C_{BW}, i.e., $T/C_{BW} = \Delta F - BW_{(drug)}/\Delta F - BW_{(vehicle)}$.

The mice were killed with CO_2 inhalation at the appropriate time point.

Pharmacokinetics

Different groups of tumor-bearing mice or rats ($n = 3$ or 4) were used for each time point with experiments set up to look at the PK in detail over 24 h or with more sparse data over 168 h. Blood (500 µl) was placed in a cold (4°C) microfuge tube using a syringe washed in an eserine–heparin mix (10 µl 200 mM eserine and 10 µl heparin) and centrifuged at 200*g*. The plasma (supernatant) was removed and stored at −20°C. Tissue samples were collected immediately after killing, weighed and placed into an equal volume of 200 mM eserine in PBS and snap-frozen in liquid nitrogen, before storing at −180°C. The esterase inhibitor eserine was used to avoid post-sampling degradation of patupilone.

Tissue samples were homogenized using an ULTRA-TURRAX homogenizer (IKA, Labortechnik, Stauffen, Germany) by 15 s bursts for a maximum of 2 min at 4°C. An internal standard (10 µl) of the structurally related epothilone (NVP-ABJ879) was added to the homogenates (250 µl or 250 mg) and after vortexing for 5 min, proteins were precipitated by the addition of a triple volume of acetonitrile. After 45 min, the protein precipitate was removed by centrifugation (10,000*g*, 5 min) and the supernatant evaporated at 40°C to dryness in a vacuum centrifuge (Speedvac, Eppendorf, Germany). The dry residue was dissolved in methanol/water (10%/90% v/v) and an aliquot of 10 µl was used for high-pressure liquid chromatography/mass spectrometry (HPLC/MS) as described previously [27].

Briefly, HPLC was performed using an autosampler (HTS PAL, CTC Analytics, CH-Zwingen) combined with a Phoenix-40 syringe pump (CE Instruments, Milan, Italy) connected to a Phenomenex C18 column, particle size 3 µm. The column eluent was introduced directly into the ion source of a single quadropole mass spectrometer (ZMD detector, Waters/Micromass, Waters Corporation, Milford, MA, USA) using as ionization technique, positive electrospray (ES). Quantitative analysis was performed by selected ion recording determined from peak to area ratios. Regression analysis used the Quanlynx/Masslynx™ software 3.4 (Micromass, Manchester, UK). The limit of quantitation was 0.0018 nmol/ml for plasma and 0.02 nmol/g for tissues.

Magnetic resonance imaging (MRI)

MRI experiments were performed on a Bruker DBX 47/30 spectrometer (Bruker BioSpin, Fällanden, CH) at 4.7T equipped with a self-shielded 12 cm bore gradient system as previously described [28]. Mice were positioned on a cradle in a supine position inside the 30-cm horizontal bore magnet and were anesthetised using 1.5% isoflurane (Abbott, Cham Switzerland) in a 1:2 v/v mixture of O_2/N_2O

using a face mask (flow-rate: 0.7 l/min). The mouse body temperature was maintained at 37°C using a warm airflow and monitored with a rectal probe.

Dynamic contrast-enhanced MRI (DCE-MRI)

GdDOTA (gadolinium tetra-azocyclododecane-tetra-acetate, Dotarem®) was injected (0.1 mmoles/kg) for determination of tumor vascular permeability, VP (initial slope of GdDOTA uptake) and extravasion, i.e., tumor extracellular leakage space and LS (final value for GdDOTA uptake). The parameter VP is positively correlated to K^{trans}, the vascular transfer constant. After 15 min, the iron oxide particle intravascular CA, Endorem® was injected (6 mmoles/kg of iron) for determination of the tumor relative blood volume (rBVol), and the initial slope of uptake of Endorem by the tumor was used as an index of blood flow (BFI). Values shown in "Results" are in arbitrary units and the principles behind measurement of these parameters have already been fully described [28].

Data analysis and statistics

Results show the mean ± SEM or ±SD as stated in the legend. Significant changes in tumor volume and body weights between the different treatments and vehicle were assessed using one-way ANOVA. For comparison of the parameters determined by DCE–MRI, a two-tailed t test was used. Data, not normally distributed, were $\log_{10}$-transformed. Correlations between different parameters were made by determining Pearson's correlation coefficient. In all cases, the significance was set at $P < 0.05$. For the pharmacokinetic data, areas under the plasma concentration versus time curves (AUC) were calculated from the mean values by linear trapezoidal rule using non-compartmental modeling for bolus i.v. dosing (WinNonlin Standard, Version 2.1, Pharsight, USA). The half-lives ($t_{1/2}$) for elimination of patupilone from the various tissues was estimated from the slope of the regression line following a semi-$\log_{10}$ plot of the data. The maximal concentration (C_{max}) was determined by inspection of the data.

Results

Activity in vitro

Patupilone had significantly higher potency ($P < 0.01$) against the four human tumor colon cancer cell lines tested (median IC50 = 0.37 nM) in comparison to paclitaxel and another epothilone, ixabepilone (Table 1). On average, paclitaxel and ixabepilone had 6-fold and 13-fold reduced potency, respectively, against the three cell lines with absent or low P-gp levels, i.e., HCT-116, HT-29 and RKO, but the activity of these two agents against P-gp over-expressing HCT-15 cells was reduced by 900- and 300-fold, respectively. Consistent with this data, the resistance factor (RF) of patupilone was scarcely altered in the P-gp over-expressing MDR cell lines, KB-8511 and MCF-7/ADR cells, compared to the parental lines, while for paclitaxel and ixabepilone the RF was significantly ($P < 0.001$) increased in comparison to patupilone (Table 1).

Table 1 Sensitivity of human tumor cell lines in vitro to patupilone and comparison to other MTS

Cell Line	Tissue	Patupilone		Paclitaxel		Ixabepilone	
		IC50	RF	IC50	RF	IC50	RF
HCT-15[a]	Colon	0.36 ± 0.07*	NA	324 ± 100	NA	110 ± 41.5	NA
HCT-116	Colon	0.43 ± 0.09*	NA	2.60 ± 0.33	NA	6.48 ± 1.35	NA
HT-29	Colon	0.38 ± 0.17*	NA	1.65 ± 0.41	NA	5.55 ± 1.70	NA
RKO	Colon	0.28 ± 0.07*	NA	2.19 ± 0.16	NA	6.33 ± 1.90	NA
MCF-7	Breast	0.33 ± 0.01	2.4**	3.37 ± 0.37	1,630	2.33 ± 0.04	685
MCF-7/ADR[a]	Breast	0.80 ± 0.09		5,500 ± 1,260		1600 ± 185	
KB-31	Cervix	0.17 ± 0.01	0.8**	2.68 ± 0.16	274	2.70 ± 0.17	47
KB-8511[a]	Cervix	0.13 ± 0.01		735 ± 104		128 ± 15.0	

Mean ± SEM for the IC50 values (from three or four independent experiments) in nM for growth inhibition, where *signifies $P < 0.01$ compared to paclitaxel and ixabepilone (one-way ANOVA after log10-transformation of the data). The cells were exposed to drugs for 3–4 days, allowing for at least two population doublings. Cell numbers were estimated by quantification of protein content of fixed cells by methylene blue staining. RF: drug resistance factor, i.e., IC50 (resistant line)/IC50 (parental line), where **signifies $P < 0.001$ compared to paclitaxel and ixabepilone (one-way ANOVA after log10-transformation of the data)

NA not applicable

[a] High expression of P-gp

Pharmacokinetics

A single dose of patupilone (1.5–4 mg/kg) to female nude mice resulted in a very rapid wide distribution from plasma to all tissues in two different models (Fig. 1). In mice bearing s.c. HCT-15 human colon tumors (Fig. 1a), a 4 mg/kg dose gave a C_{max} (5 min) of between 1.6 ± 0.1 (muscle) and 6.8 ± 1.3 nmol/g (tumor). In the s.c. tumor and brain, this concentration was essentially unchanged over 24 h, while in muscle and liver there was a slow elimination with estimated half-lives of 10–12 h. Overall exposure ($AUC_{0-24\ h}$) was greatest in the tumor and brain, which was significantly greater than the other tissues ($P < 0.001$), and the tumor-AUC was also significantly greater than the brain-AUC ($P < 0.001$); see Table 2. Similar data were obtained in the second nude mouse model (human HT-29 colon tumors) in which two different doses of patupilone were compared over 1 week post single-dose patupilone administration (Table 2). Again, plasma elimination was very rapid, while the slowest elimination was from tumor with essentially no concentration change over the first 24 h, see Fig. 1b and inset. Over 24 h, the half-lives in the liver and muscle were not significantly different from those in the HCT-15 model where a higher dose was used (Table 2), and overall exposure (AUC_{0-168} μM h) also indicated dose-proportional pharmacokinetics for patupilone with tumor > liver > muscle ($P < 0.01$ tumor versus muscle), and tumor and small intestine showing similar exposure.

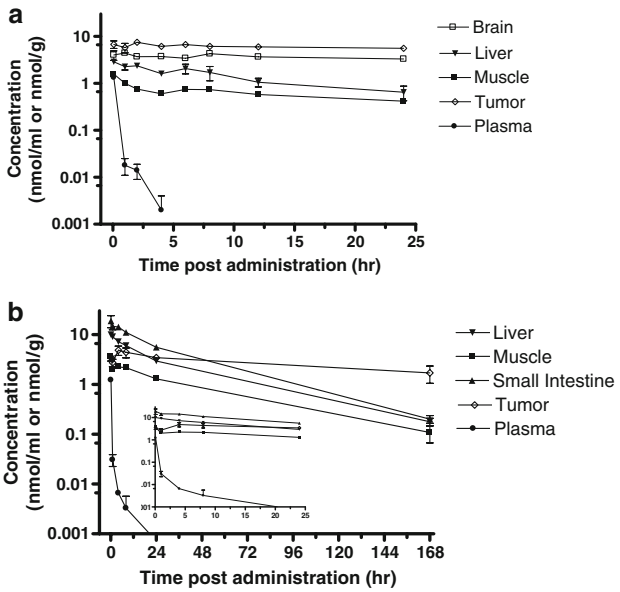

Fig. 1 Pharmacokinetics of patupilone in female nude mice bearing s.c. human colon adenocarcinomas following a single bolus i.v. administration. Female BALB/c (HCT-15 tumors) or Harlan (HT-29 tumors) bearing s.c tumors of approximately 300 mm^3 were administered a single i.v. dose of patupilone (4 or 2.5 mg/kg, respectively). Inset to **b** shows the same data plotted over 24 h. The mice were killed at different times after administration. The blood, tumors and other tissues were collected and processed for the determination of patupilone levels by HPLC–MS, as described in "Materials and methods". Data show the mean ± SEM

Table 2 Summary of patupilone pharmacokinetics in female nude mice bearing the s.c. human colon adenocarcinomas HCT-15 and HT-29

A					
Patupilone single i.v. dose (mg/kg)	PK parameter	Liver	Muscle	Brain	HCT-15 tumor
4	$C_{5\ min}$ μM	2.9 ± 0.1	1.6 ± 0.1	4.0 ± 1.0	6.8±1.3
	$T_{1/2}$ h	11.7 ± 1.6	9.8 ± 7.7	NA	NA
	AUC_{0-24} μM h	31.9 ± 6.1	14.8 ± 1.2	88.1 ± 3.3	145.6±5.3**
B					
Patupilone single i.v. dose (mg/kg)	PK parameter	Liver	Muscle	Small intestine	HT-29 tumor
1.5	$C_{5\ min}$ μM	9.9 ± 0.5	3.2 ± 0.1	10.6 ± 3.7	1.6 ± 0.2
	$T_{1/2}$ h	10.9 ± 1.9	16.5 ± 5.1	11.8 ± 3.8	NA
	AUC_{0-168} μM h	252 ± 14	109 ± 7	304 ± 56	331 ± 66*
2.5	$C_{5\ min}$ jM	10.0 ± 0.5	3.7 ± 0.5	19.0 ± 5.1	3.6 ± 0.6
	$T_{1/2}$ h	14.1 ± 1.0	21.9 ± 14.3	14.7 ± 1.6	NA
	AUC_{0-168} μM h	358 ± 19	147 ± 10	660 ± 72	468 ± 30*

Mean values ($n = 4$) for the various PK parameters derived ("Materials and methods") from the data shown in Fig. 1 for (A) mice, bearing s.c. HCT-15 tumors, treated with a single i.v. bolus dose of patupilone (4 mg/kg). **$P < 0.001$ indicates significant difference from the other tissues. (B) Mice, bearing s.c. HT-29 tumors, treated with a single i.v. bolus dose of patupilone (1.5 or 2.5 mg/kg)

* $P < 0.01$ indicates significant difference from muscle. Note, to permit comparison between A and B, the $T_{1/2}$s were calculated over 24 h (see "Results")

When the half-lives were estimated in the HT-29 model over 168 h, the values increased two to threefold in all tissues measured, suggesting a secondary elimination phase. The patupilone concentration detected in tumors remained above 2 μM for at least 24 h.

A similar pharmacokinetic pattern was observed in two different rat s.c. syngeneic tumor models using CA20498 pancreatic tumors in Lewis rats (Fig. 2a) and A15 glioma tumors in BDix rats (Fig. 2b). Again, patupilone was rapidly eliminated from plasma, but scarcely at all from brain and tumor with slower elimination from liver, muscle and skin. In these rat models, overall exposure was greatest in the small intestine ($P < 0.001$ versus the other tissues) with gut >> liver > muscle ≅ tumor > brain in Fisher rats and gut > tumor > skin in BDix rats ($P < 0.01$). Thus, relative exposure of patupilone in the gut was greater for rats than mice, an observation that may explain why patupilone treatment in rats, but not mice, was associated with diarrhea. Several other rat and mouse tumor-bearing models confirmed substantial uptake and retention of patupilone by s.c. tumors and the brain with minimal elimination after several days. Furthermore, distribution studies in both mice and rats with ^{14}C-patupilone confirmed uptake in the brain with highest concentrations in the pineal and pituitary glands (data not shown).

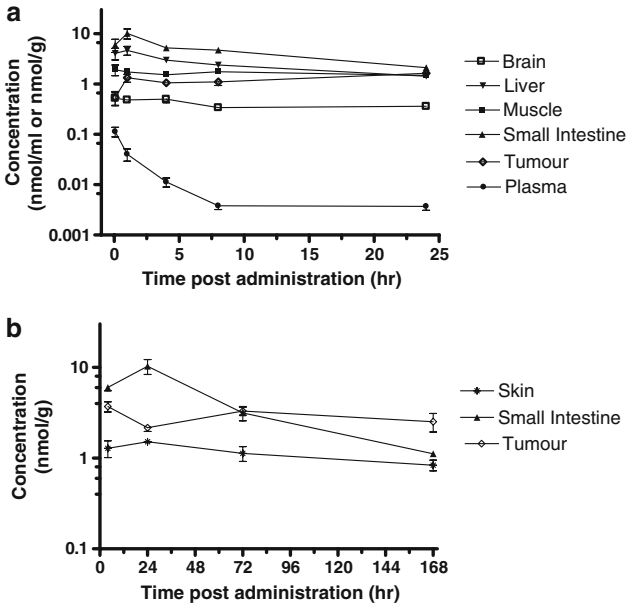

Fig. 2 Pharmacokinetics of patupilone in female rats bearing s.c. rat pancreatic tumors (**a**) and glioma tumors (**b**) following a single bolus i.v. administration. Male Lewis rats (CA20498 pancreatic tumors) or female BDix rats (A15 glioma tumors) bearing s.c tumors of at least 300 mm^3 were administered a single i.v. dose of patupilone (1.5 mg/kg). The rats were killed at different times after administration, the blood, tumors and other tissues were collected and processed for the determination of patupilone levels by HPLC–MS, as described in "Materials and methods". Data show the mean ± SEM

Activity in vivo

Patupilone inhibited growth of HCT-15 tumors (high P-gp expression) giving at the endpoint a T/C_{TVol} of 0.3 and −0.03 for the doses of 4 mg/kg once and 2.5 mg/kg qw, respectively, while paclitaxel (15 mg/kg q2d) was without any significant effect ($T/C_{TVol} = 0.69$). Treatment with paclitaxel was well tolerated, causing no significant body weight loss, while the patupilone treatments caused transient body weight loss followed by recovery after cessation of treatment (Fig. 3a b, Table 3). Similar efficacy and tolerability of patupilone was observed in the HT-29 s.c. tumor model, but in this tumor, which does not show high P-gp expression, paclitaxel showed strong activity causing tumor regression (Table 3) and a similar pattern was seen in the HCT-116 s.c. tumor model (Table 3).

Thus, these observations in vivo using three different human colon tumor xenograft models were consistent with the experiments in vitro. Similarily, patupilone caused regression of both the parental KB-31 cervical tumors, $T/C_{Tvol} = -0.35$ (Fig. 3c) and the mutant P-gp over-expressing KB-8511 tumors, $T/C_{Tvol} = -0.1$ (Fig. 3e), while paclitaxel was only active against the parental KB-31 tumors. Furthermore, in another MDR-model pair, patupilone produced minor, but durable, regressions in s.c MCF-7 tumors and essentially stable disease in orthotopic MCF-7/ADR tumors (data not shown).

Using the HT-29 model, we investigated the role of tumor size at the start of treatment on tumor uptake of patupilone and subsequent activity. Figure 4a shows that patupilone (2.5 mg/kg qw) efficacy was the same against tumors of 100 or 500 mm^3 resulting in a final T/C_{TVol} of 0.21 and 0.24 for small and large tumors, respectively. Similar data (not shown) was obtained using the KB-8511 model with large (300 ± 38 mm^3) and small (120 ± 6 mm3) tumors giving similar T/C_{TVol} of −0.15 and −0.05, respectively, in response to a single dose of patupilone. Representative T_1-weighted MRI images of untreated small (115 ± 10 mm^3, $n = 8$) and large (503 ± 58 mm^3, $n = 8$) HT-29 tumors are shown in Fig. 4b and c, respectively. Images were made following injection of GdDTPA for DCE-MRI measurement of tumor vascular permeability (VP) prior to drug treatment, which shows that perfusion was limited mostly to the rim in large tumors, but was more homogeneous in small tumors. A similar result was obtained following injection of the intravascular CA, Endorem, for measurement of relative blood volume (rBVol) and blood flow index (BFI). The DCE-MRI studies showed that large tumors had a significantly smaller blood volume ($P < 0.001$) and blood flow index ($P < 0.05$), the latter being uniformly low in comparison to small tumors as shown in Fig. 4d and e. Indeed, tumor volume was significantly negatively correlated with rBVol ($R = -0.56$,

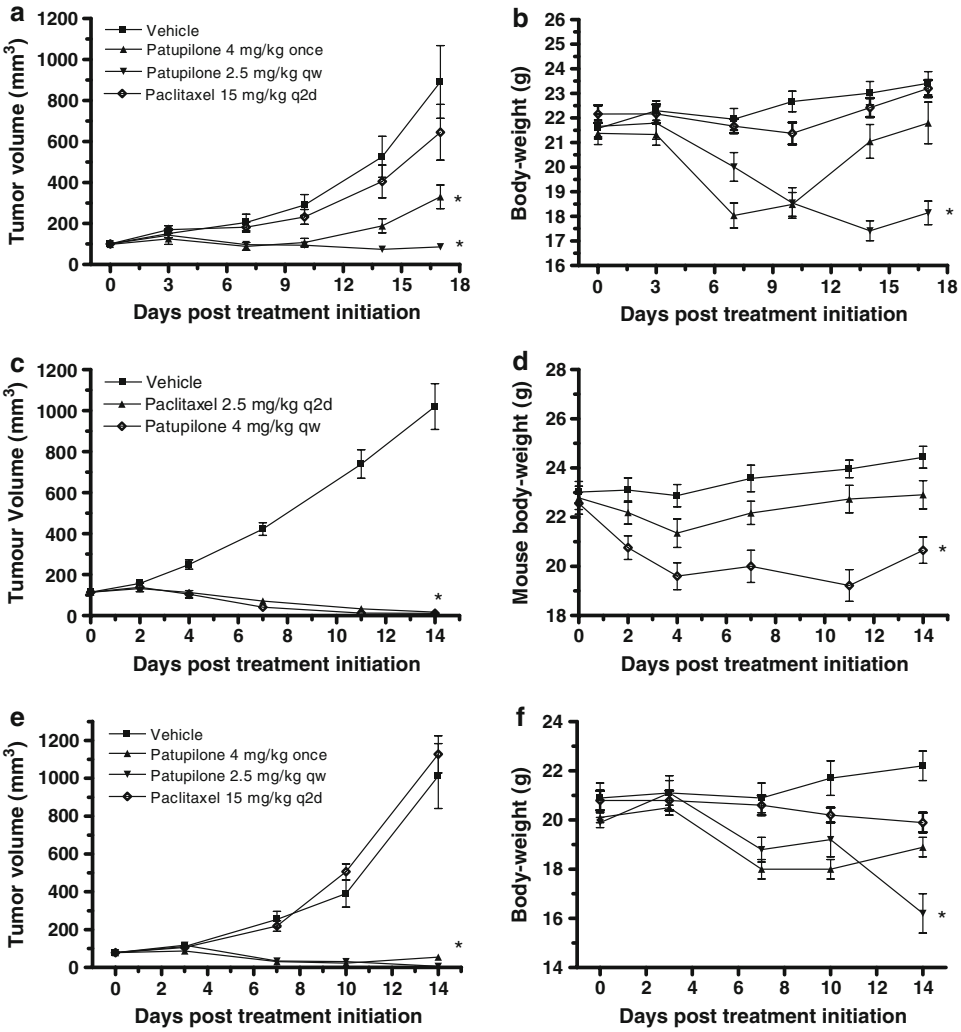

Fig. 3 Efficacy and tolerability of patupilone in female nude mice bearing different s.c. human tumors and comparison with paclitaxel. Female BALB/c mice bearing different s.c. tumors, HCT-15 (**a**, **b**), KB-31 (**c**, **d**) and KB-8511 (**e**, **f**), were administered patupilone-vehicle or using optimal regimens at near maximally tolerated doses, patupilone or paclitaxel. Tumor volumes and body weights were periodically measured. Data show mean ± SEM, where * $P < 0.05$ versus vehicle-control using a one-way ANOVA at the endpoint

$P = 0.036$, $n = 14$), and there was a trend for a similar correlation with BFI ($R = -0.49$, $P = 0.093$, $n = 13$). Despite these clear differences in tumor vascularity between small and large tumors, drug levels of patupilone in the tumors 24 h after a single dose of 2.5 mg/kg were effectively the same at 0.53 ± 0.13 μM and 0.59 ± 0.10 μM for large and small tumors, respectively. There were no significant differences in patupilone plasma levels or the tumor LS or VP between small and large tumors ($P > 0.4$; results not shown).

Discussion

Our results demonstrate that the microtubule stabilizer, patupilone (epothilone B) is a potent inhibitor of human colon cancer cell growth, whether grown in culture or as solid tumor xenografts in nude mice. Furthermore, potency is maintained in multi-drug-resistant colon cancer cells reported to express the P-gp drug-efflux pump. In contrast, the taxane paclitaxel, which has the same molecular target as patupilone, was less potent in vitro and its activity was markedly reduced in three different cell lines with high endogenous P-gp expression. In addition, although patupilone and paclitaxel had comparable activity in vivo at tolerable doses in paclitaxel-sensitive models (HT-29, KB-31, HCT-116), paclitaxel was without significant activity in vivo in models known to over-express the P-gp drug-efflux pump (HCT-15 and KB-8511). The epothilone B derivative, ixabepilone, also displayed reduced potency in vitro and its activity was also affected by P-gp expression, although less so than paclitaxel. Similar data showing reduced activity in vitro of paclitaxel and ixabepilone using MCF-7 cell lines differentially expressing P-gp were reported by Klar et al. [29].

P-gp has for many years been discussed as an important means of both intrinsic and acquired drug resistance and has often been cited as an independent prognostic indicator of survival [30, 31]. However, its role in specific resistance to the taxanes is not clear, since it is likely that additional

Table 3 Efficacy and tolerability of patupilone in comparison to paclitaxel in female nude mice bearing s.c. human colon adenocarcinomas

Treatment and schedule	Tumor response			Host response		
	TVol (mm^3)	ΔTVol (mm^3)	T/C_{TVol}	BW (g)	Δ%BW (g)	T/C_{BW}
HCT-15[a]						
Vehicle 10 ml/kg qw	891 ± 177	791 ± 170	1.00	24.4 ± 0.5	8.5 ± 1.3	1.00
Patupilone 4 mg/kg once	330 ± 58	232 ± 56	0.29*	21.8 ± 0.8	2.1 ± 3.7	0.94
Patupilone 2.5 mg/kg qw twice	76 ± 15	−25 ± 15	−0.03*	18.1 ± 0.5	−17.3 ± 1.7*	0.76*
Paclitaxel 15 mg/kg q2d five-times	645 ± 136	545 ± 133	0.69	23.2 ± 0.3	4.7 ± 0.7	0.97
HT-29[b]						
Vehicle 10 ml/kg qw	436 ± 113	343 ± 104	1.00	21.4 ± 0.4	2.9 ± 1.5	1.00
Patupilone 3 mg/kg once	198 ± 42	94 ± 33	0.27	22.3 ± 0.4	3.8 ± 0.6	1.01
Patupilone 2.5 mg/kg qw twice	83 ± 15	−12 ± 6	−0.03*	18.3 ± 0.5	−12.8 ± 1.9	0.85*
Patupilone 2 mg/kg qw twice	176 ± 31	81 ± 22	0.24	18.3 ± 0.6	−13.4 ± 2.1	0.84*
Paclitaxel 15 mg/kg q2d five-times	9 ± 4	−86 ± 8	−0.25*	21.0 ± 0.2	0.8 ± 0.9	0.98
HCT-116[c]						
Vehicle 10 ml/kg qw	971 ± 229	880 ± 223	1.00	20.8 ± 0.5	−1.4 ± 0.4	1.00
Patupilone 2.5 mg/kg qw twice	355 ± 77	263 ± 71	0.3*	16.3 ± 0.3	−25.9 ± 1.2	0.74*
Paclitaxel 15 mg/kg q2d five-times	233 ± 37	141 ± 29	0.16*	18.0 ± 0.6	−18.3 ± 2.1	0.82*

[a] HCT-15 tumors were created as described in "Materials and methods" and were treated 6 days after transplantation with the schedules shown. Results show the mean ± SEM ($n = 8$ mice) 17 days after treatment initiation, where * $P < 0.05$, compared to vehicle using Dunnett's or Dunn's one-way ANOVA following log-transformation of the data

[b] HT-29 tumors were created as described in "Materials and methods" and were treated 8 days after transplantation with the schedules shown. Results show the mean±SEM ($n = 8$ mice) 16 days after treatment initiation, where * $P < 0.05$, compared to vehicle using Dunnett's or Dunn's one-way ANOVA following log-transformation of the data

[c] HCT-116 tumors were created as described in "Materials and methods" and were treated 10 days after transplantation with the schedules shown. Results show the mean ± SEM ($n = 8$ mice) 14 days after treatment initiation, where * $P < 0.05$, compared to vehicle using Dunnett's or Dunn's one-way ANOVA following log-transformation of the data

factors are involved, e.g., other pump- or metabolism-mediated mechanisms reducing intracellular drug levels [32], changes in the molecular target such as point mutations in β-tubulin [9] or in the relative expression of different β-tubulin isotypes [33], post-translational modification of β-tubulin and activity of various microtubule regulatory proteins [34], and ultimately also changes in the pathways leading to apoptosis [35]. Despite these possibilities, a drug that is a priori unaffected by P-gp expression and shows potent anti-tumor activity at tolerable doses should create new opportunities in cancer indications such as CRC, brain tumors and RCC, which have proved inaccessible to the taxanes or ixabepilone. Indeed, significant activity for patupilone was reported in phase-I clinical trials for CRC and phase-II trial for RCC, indications where the taxanes [14, 16] and also ixabepilone [13, 36] have little or no activity.

The pharmacokinetics of patupilone showed that in both mice and rats the drug is rapidly and widely distributed to tissues, and, more importantly, remains in both tumor and brain with no measurable decrease in drug levels in the tumor at 7 days post treatment. Thus, not only can patupilone cross the blood–brain barrier, but it also can persist there suggesting that activity against brain tumors is possible. Tumor patupilone levels were >2 μM for at least 24 h following administration, an order of magnitude in excess of the accumulation-driven cellular concentration (200 nM) that had been observed in vitro 24 h after a 2-h incubation of HeLa/KB-31 cells with 1 nM patupilone [7], a medium concentration above the antiproliferative IC50 for these and all other cell lines tested here, including HT-29. Apart from tumor, patupilone exposure was highest in the gut and appeared to be greater in rats than in mice, perhaps accounting for the dose-dependent diarrhea observed in Lewis and BDix rats but rarely seen in mice [37].

The DCE-MRI data showed that large HT-29 xenografts had significant differences in the functional vasculature as compared to small tumors. Other pre-clinical investigations have shown that large tumors have blood flow rates lower than small tumors [38, 39], and consequently can show greater hypoxia [40]; but exceptions do occur [41] and the relationship of size and flow rate may not always be linear at smaller tumor volumes [39]. Nevertheless in this study, we detected significant differences in tumor blood volume and blood flow between small and large HT-29 tumors, although the mean concentration of patupilone in both tumor types was the same at 24 h post injection; a time point representing a steady state for patupilone elimination from tumors, and indeed this led to similar anti-tumor

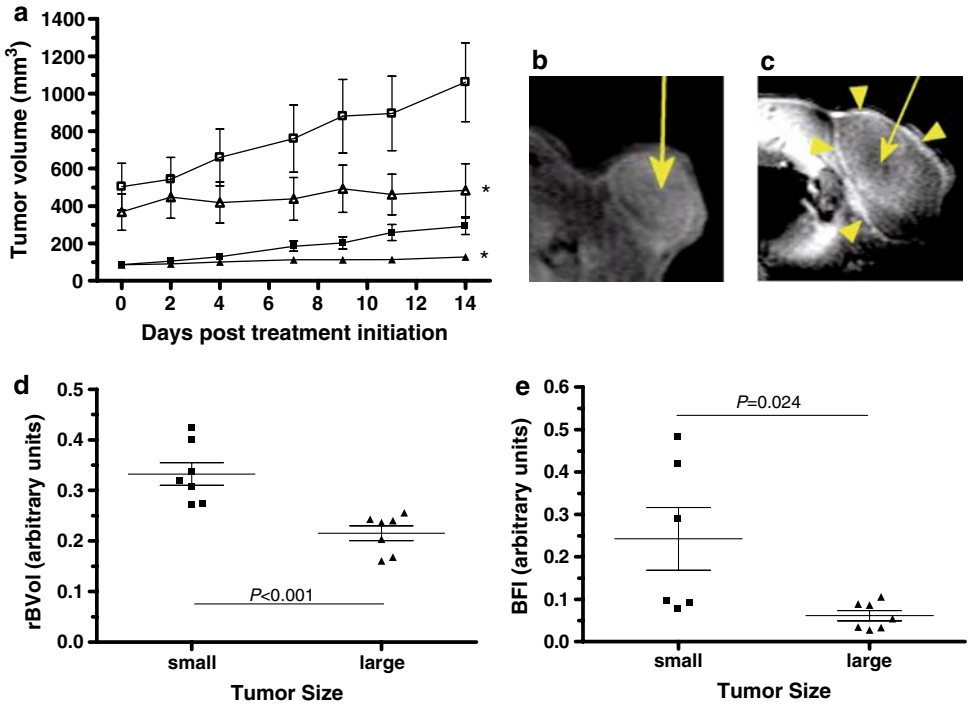

Fig. 4 Tumor size, blood volume, flow and patupilone concentrations and efficacy in female nude mice bearing s.c. HT-29 tumors. HT-29 tumors were created by s.c. injection of 5×10^6 cells in PBS in Harlan nude mice and tumor volumes were determined using calipers as described in "Materials and methods". All results show mean ± SEM (**a**) Comparison of efficacy of 2.5 mg/kg qw patupilone (*open* and *closed triangles*) versus vehicle (*open* and *closed squares*) against small and large tumors, where * $P < 0.02$ versus respective vehicle (two-tailed *t* test). **b**, **c** T_1 weighted MR images of HT-29 tumors (*arrows*) showing small, **b** 4.4 mm × 3.4 mm and large, **c** 9.8 mm × 5.2 mm tumors. Images were taken at the end of a DCE-MRI experiment measuring permeability (VP), but before drug treatment. GdDOTA extravasation at the end of the permeability measurement in large tumors was greatest at the tumor rim (*arrowheads*), but more heterogeneous in the small tumors. **d**, **e** Relative tumor blood volume (rBVol) and blood flow index (BFI) in small and large tumors determined from DCE-MRI measurements of tumor uptake of the contrast agents GdDTPA and Endorem, respectively (see "Materials and methods"). Statistical comparisons were by a two-tailed *t* test where * significant difference ($P < 0.05$)

efficacy. Thus, a minimal vascularity may be sufficient for patupilone to gain access to the solid tumor after which diffusion is sufficient to deliver the drug to the rest of the tumor. Since solid tumors in the clinic have been shown to display a rather chaotic vasculature with low perfusion and permeability leading to a high interstitial fluid pressure [42], the data imply that patupilone could still enter the tumor space and cause significant inhibition of tumor growth.

In conclusion, we have demonstrated that patupilone is more potent than other MTS and this anti-cancer activity is unaffected by the P-gp pump both in vitro and in vivo. Patupilone shows a rapid wide tissue distribution, including the brain and s.c. tumors where there is little or no elimination over several days. Furthermore, tumor penetration is unaffected by the degree of tumor vascularity and thus the drug shows equal activity against both small as well as large poorly vascularized tumors. These data suggest that patupilone may prove to have important clinical efficacy in indications where other MTS have until now failed.

Acknowledgments We thank Mike Becquet, Mark Hattenberger, Melanie Muller, Samuel Kunz, Fabienne Schaeffer, Julian Vaxelaire, Robert Reuter and Jacqueline Loretan for their excellent technical support.

References

1. Hoefle G, Steinmetz H, Bedorf N, Schomberg D, Gerth K, Reichenbach H (1996) Epothilone A and B - novel 16-membered macrolides with cytotoxic activity: isolation, crystal structure, and conformation in solution. Angew Chem Int Ed Engl 35:1567–1569
2. Buey RM, Diaz JF, Andreu JM et al (2004) Interaction of epothilone analogs with the paclitaxel binding site: relationship between binding affinity, microtubule stabilization, and cytotoxicity. Chem Biol 11:225–236
3. Reese M, Sanchez-Pedregal VM, Kubicek K et al (2007) Structural basis of the activity of the microtubule-stabilizing agent epothilone A studied by NMR spectroscopy in solution. Angew Chem Int Ed Engl 46:1864–1868
4. Bollag DM, McQueney PA, Zhu J et al (1995) Epothilones, a new class of microtubule-stabilizing agents with a taxol-like mechanism of action. Cancer Res 55:2325–2333
5. Broker LE, Huisman C, Span SW, Rodriguez JA, Kruyt FA, Giaccone G (2004) Cathepsin B mediates caspase-independent cell

death induced by microtubule stabilizing agents in non-small cell lung cancer cells. Cancer Res 64:27–30
6. Ferretti S, Allegrini PR, O'Reilly et al (2005) Patupilone induced vascular disruption in orthotopic rodent tumor models detected by magnetic resonance imaging and interstitial fluid pressure. Clin Cancer Res 11:7773–7784
7. Wartmann M, Altmann K-H (2002) The Biology and Medicinal Chemistry of Epothilones. Curr Med Chem – Anti-Cancer Agents 2:123–148
8. Tanabe KM, Millward M, Allen JD (2005) Interactions of patupilone (epothilone B) with multidrug transporter proteins. Proceedings of the 96th annual meeting AACR, Ananheim, CA; Apr 16–20, p. 809
9. Giannakakou P, Sackett DL, Kang YK (1995) Paclitaxel-resistant human ovarian cancer cells have mutant beta-tubulins that exhibit impaired paclitaxel-driven polymerization. J Biol Chem 272:17118–17125
10. Thorpe PE (2004) Vascular targeting agents as cancer chemotherapeutics. Clin Cancer Res 10:415–427
11. Bocci G, Nicholaou KC, Kerbel RS (2002) Protracted low-dose effects on human endothelial cell proliferation and survival in vitro reveal a selective anti-angiogenic window for various drugs. Cancer Res 62:6938–6943
12. Woltering EA, Lewis JM, Maxwell PJ et al (2003) Development of a novel in vitro human tissue-based angiogenesis assay to evaluate the effect of antiangiogenic drugs. Annals of Surgery 237:790–798
13. Goodin S, Kane MP, Rubin EH (2004) Epothilones: mechanism of action and biologic activity. J Clin Oncol 22:2015–2025
14. O'Neil BH, Goldberg RM (2005) Chemotherapy for advanced colorectal cancer: let's not forget how we got here (until we really can). Semin Oncol 32:35–42
15. Melichar B, Casado Er, Tabernero J, et al. Patupilone in chemotherapy-pretreated patients with advanced colorectal cancer (CRC) receiving nutritional support and intensive diarrea management: a phase I multicenter trial. Ann Oncol 2006; 17 (Supplement 9), Abstract 31st ESMO congress
16. Kretzschmar A, Kohne CH, Dorken B (1997) Docetaxel in treatment of other solid tumors. Med Klin (Munich) 92(Suppl 4):16–22
17. Sharma N, Ramachandran S, Bowers M et al (2000) Multiple factors other than p53 influence colon cancer sensitivity to paclitaxel. Cancer Chemother Pharmacol 46:329–337
18. Goldstein LJ (1996) MDR1 gene expression in solid tumors. Eur J Cancer 32A:1039–1050
19. Schinkel AH, Jonker JW (2003) Mammalian drug efflux transporters of the ATP binding cassette (ABC) family: an overview. Adv Drug Delivery Rev 55:3–29
20. Blobe GC, Sachs CW, Khan WA, Fabbro D, Stabel S, Wetsel WC, Obeid LM, Fine RL, Hannun YA (1993) Selective regulation of protein kinase C (PKC) isoenzymes in multidrug-resistant MCF-7 cells. J Biol Chem 268:658–664
21. Masters JR (2002) HeLa cells 50 years on: the good, the bad and the ugly. Nature Rev 2:315–319
22. Akiyama S, Fojo A, Hanover JA, Pastan I, Gottesman MM (1985) Isolation and genetic characterization of human KB cell lines resistant to multiple drugs. Somatic Cell and Molecular Genetics 11:117–126
23. Wu L, Smythe AM, Stinson SF, Mullendore LA, Monks A, Scudiero DA, Paull KD, Koutsoukos AD, Rubinstein LV, Boyd MR et al (1992) Multidrug-resistant phenotype of disease oriented panels of human tumor cell lines used for anticancer drug screening. Cancer Res 52:3029–3034
24. Meyer T, Regenass U, Fabbro D, Alteri E, Rösel J, Müller M, Caravatti G, Matter A (1989) A derivative of staurosporine (CGP 41 251) shows selectivity for protein kinase C inhibition and in vitro anti-proliferative as well as in vivo antitumor activity. Int J Cancer 43:851–856
25. Boulay A, Zumstein-Mecker S, Stephan C et al (2005) Antitumor efficacy of intermittent treatment schedules with the rapamycin derivative RAD001 correlates with prolonged inactivation of ribosomal protein S6 kinase 1 in peripheral blood mononuclear cells. Cancer Res 64:252–261
26. O'Reilly T, McSheehy PM, Wenger F, Hattenberger M, Muller M, Vaxelaire J, Altmann KH, Wartmann M (2005) Patupilone (epothilone B, EPO906) inhibits growth and metastasis of experimental prostate tumors in vivo. Prostate 65:231–240
27. Blum W, Aichholz R, Ramstein P, Kühnol J, Brüggen J, O'Reilly T, Flörsheimer A (2001) In vivo metabolism of epothilone B in tumor-bearing nude mice: identification of three new epothilone B metabolites by capillary high-pressure liquid chromatography/mass spectrometry/tandem mass spectrometry. Rapid Commun Mass Spectrom 15(1):41–49
28. Traxler P, Allegrini PR, Brandt R et al (2004) AEE788: a dual family epidermal growth factor receptor/ErbB2 and vascular endothelial growth factor receptor tyrosine kinase inhibitor with antitumor and antiangiogenic activity. Cancer Res 64:4931–4941
29. Klar U, Buchmann B, Schwede W et al (2006) Total Synthesis and Antitumor Activity of ZK-EPO: The First Fully Synthetic Epothilone in Clinical Development. Angew Chem 45:7942–7948
30. Khalifa MA, Abdoh AA, Mannel RS et al (1997) P-glycoprotein as a prognostic indicator in pre- and post-chemotherapy ovarian carcinoma. Int J Gyn Path 16:69–75
31. Penson RT, Oliva E, Skates SJ et al (2004) Expression of multidrug resistance-1 protein inversely correlates with paclitaxel response and survival in ovarian cancer patients: a study in serial samples. Gyn Onc 93:98–106
32. Hinoshita E, Uchiumi T, Taguchi K, Kinukawa N, Tsuneyoshi M, Maehara Y, Sugimachi K, Kuwano M (2000) Increased expression of an ATP-binding cassette superfamily transporter, multidrug resistance protein 2, in human colorectal carcinomas. Clin Cancer Res 6:2401–2407
33. Kamath K, Wilson L, Cabral F, Jordan MA (2005) BetaIII-tubulin induces paclitaxel resistance in association with reduced effects on microtubule dynamic instability. J Biol Chem 280(13):12902–12907
34. Pellegrini F, Budman DR (2005) review: tubulin function, action of antitubulin drugs and new drug development. Cancer Invest 23:264–273
35. Morse DL, Gray H, Payne CM, Gillies RJ (2005) Docetaxel induces cell death through mitotic catastrophe in human breast cancer cells. Mol Cancer Ther 4(10):1495–1504
36. Eng C, Kindler HL, Nattam S et al (2004) A phase-II trial of the epothilone B analog, BMS-247550, in patients with previously treated advanced colorectal cancer. Ann Oncol 15:928–932
37. Saulnier M, Roman D, Mahl A et al (2003) Integrative toxicological and pharmacogenomic investigations of intestinal effects induced by epothilone B after single intraveneous administration in rats. Clin Cancer Res 9(16, part 2):A270
38. Siracka E, Pappova N, Pipa V, Durkovsky J (1979) Changes in blood flow of growing experimental tumor determined by the clearance of 133Xe. Neoplasma 26:173–177
39. Sevick EM, Jain RK (1989) Geometric resistance to blood flow in solid tumors perfused ex vivo: effects of tumor size and perfusion pressure. Cancer Res 49:3506–3512
40. McSheehy PMJ, Robinson SP, Ojugo ASE et al (1998) Carbogen breathing increases 5-fluorouracil uptake and cytotoxicity in hypoxic murine tumours: a magnetic resonance study in vivo. Cancer Res 58:1185–1194
41. Casillas S, Dietz DW, Brand MI, Jones SC, Vladisavljevic A, Milsom JW (1997) Perfusion to colorectal cancer liver metastases is not uniform and depends on tumor location and feeding vessel. J Surg Res 67:179–185
42. Jain RK (2001) Normalizing tumor vasculature with anti-angiogenic therapy: a new paradigm for combination therapy. Nat Med 7:987–989